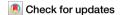
Published in partnership with the Parkinson's Foundation



https://doi.org/10.1038/s41531-025-01091-z

Elevated plasma levels of alpha-synuclein are dispensable for Parkinson's disease pathology



Jin-Young Jeong^{1,2,4}, Namsuk Kim^{1,4}, Yan Li¹, Doo-Jin Kim³, Hyong Kyu Kim³ & Won-Jong Oh¹ ⊠

Although α -synuclein levels are elevated in the blood plasma of Parkinson's disease (PD) patients, it remains unclear whether blood-derived α -synuclein directly contributes to PD. To investigate this, we developed a novel mouse model in which human α -synuclein levels are increased in the blood. Despite a significant increase in α -synuclein in the blood, no noticeable behavioral abnormalities were observed in aged mice. Additionally, we did not observe plasma α -synuclein aggregation in the blood or entry of human α -synuclein into the brain. These results suggest that elevated blood levels of α -synuclein may not be sufficient to induce PD progression.

Parkinson's disease (PD) is characterized by various types of damage to neurons in the aged brain, particularly a selective loss of dopaminergic neurons in the substantia nigra¹. Besides direct neuronal damage caused by toxic α-synuclein, vascular structural and functional impairments are crucial etiologic factors in the progression of PD². Various vasculature-related pathological changes, including alterations in blood flow, disruption of the blood-brain barrier (BBB) and abnormal angiogenesis, have been observed in multiple animal models, as well as in individuals with PD³⁻⁷. Thus, there are two distinct views regarding the mechanistic links between cerebrovascular dysfunction and PD progression. The first perspective is the vascular-to-neuronal view, which postulates that cerebrovascular abnormalities such as stroke and infectious disease cause neuronal damage prior to apparent PD symptoms, likely through an increase in vascular permeability, enhancement of neuroinflammation and subsequent accumulation of toxic α-synuclein in neurons^{8,9}. The second is the neuro-to-vascular view, which suggests that toxic α-synuclein originating from neurons impacts vascular structure and function, thereby forming a vicious cycle that accelerates neuronal damage in the brain 10,111.

A significant body of evidence has shown that α -synuclein is also expressed in other peripheral tissues, including vascular cells and erythropoietic lineage cells 12,13 . α -synuclein in the blood is predominantly stored in red blood cells (RBCs) 14 . Furthermore, despite inconsistent findings on plasma and cerebrospinal fluid α -synuclein levels in PD patients, a recent meta-analysis of 32 published articles reported a significant increase in blood total α -synuclein levels in PD patients compared to control subjects 15 . Another intriguing matter pertains to the presence and origin of toxic α -synuclein, particularly its oligomeric form, in the bloodstream. In

PD patients, the oligomeric form of α -synuclein has been detected in red blood cells as well as blood samples^{16,17}. Notably, these oligomeric forms originate from the central nervous system, and some are found encapsulated in extracellular vesicles in blood¹⁸. Nonetheless, it remains unclear whether elevation of α -synuclein levels in the blood can lead to the generation of toxic aggregates, promote the passage of α -synuclein across the BBB, or persistently cause neuronal impairments, ultimately contributing to the progression of PD.

To enable efficient extracellular secretion of α-synuclein, we generated secretable human α -synuclein by adding a modified albumin signal peptide to the N-terminus, which is cleaved within the endoplasmic reticulum during conventional secretory processing (Supplementary Fig. 1a)¹⁹. Upon transfection into human hepatoma HepG2 cells, the secreted form of αsynuclein (hSNCAse) exhibited efficient extracellular secretion, while the non-secreted form (hSNCA) showed minimal levels in the culture media (Supplementary Fig. 1b). To investigate whether the secreted human αsynuclein can enter the brain endothelial cells, we introduced conditioned media containing human α-synuclein to cultured mouse brain endothelial cells (bEnd.3). Endothelial cells exhibited uptake of secreted human αsynuclein after 2 h of incubation, contrasting with low levels of uptake observed in conditioned media from non-secretable human α-synucleintransfected HepG2 cells (Supplementary Fig. 1c, d). These results suggest that α -synuclein with a signal peptide can be efficiently secreted into the extracellular space and delivered to endothelial cells.

Next, we developed a novel mouse model (hSNCA^{se} mice) using the CRISPR/Cas9 system. We inserted the secretable human α -synuclein construct after the CAG promoter and the floxed stop cassette of the ROSA26

¹Neurovascular Biology Laboratory, Neurovascular Unit Research Group, Korea Brain Research Institute, Daegu, Republic of Korea. ²Department of Brain Sciences, Daegu Gyeongbuk Institute of Science and Technology, Daegu, Republic of Korea. ³Biomedical Research Institute, Chungbuk National University Hospital, Cheongju, Republic of Korea. ⁴These authors contributed equally: Jin-Young Jeong, Namsuk Kim.

□ Parkinson's Foundation

allele, allowing for the induction of human α -synuclein extracellular secretion in a time- and space-dependent manner (Fig. 1a). To specifically increase α -synuclein levels in the blood, we crossed hSNCA^{se} mice with albumin-CreERT2 mice, in which Cre recombinase is activated in hepatocytes through tamoxifen injection (Fig. 1b)²⁰. A single injection of tamoxifen (0.1 mg/g) at 4 months of age significantly increased human α -synuclein

expression in hepatocytes and subsequently in blood, whereas vehicle injection did not (Fig. 1c, d).

To examine whether the elevated α -synuclein levels induce PD-related behavioral phenotypes, we maintained the mice for 5 months after the initiation of α -synuclein secretion at 4 months of age and performed several behavioral assays that specifically focused on motor function, such as wire

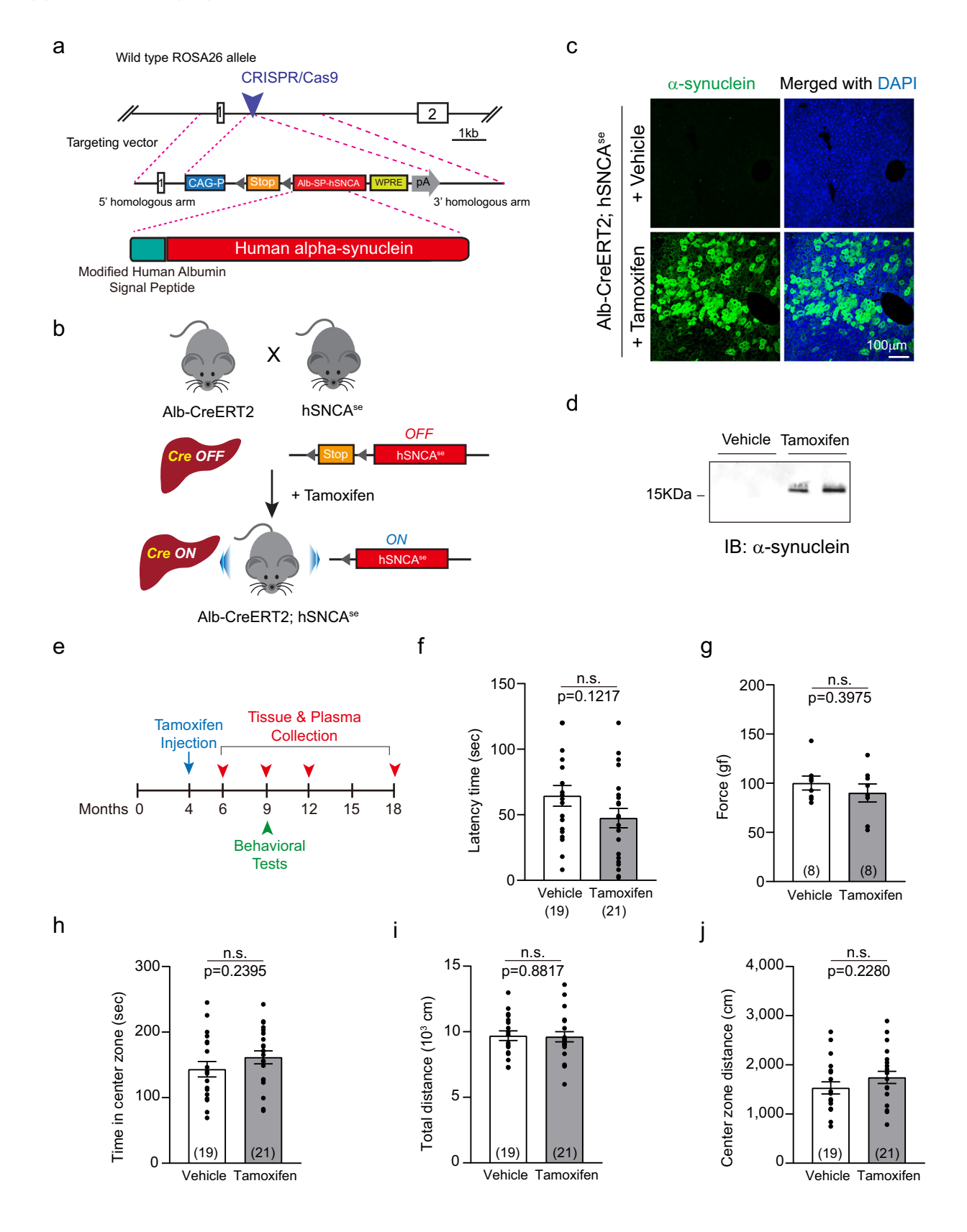


Fig. 1 | Specific elevation of human α -synuclein in the blood using Alb-CreERT2; hSNCAse mice does not induce motor behavioral deficits. a Schematic representation of the targeting vector design and homologous recombination strategy for insertion of the hSNCAse construct at the ROSA26 locus. b Mouse breeding scheme for hepatocyte-specific expression of secretable human α -synuclein. c Representative image showing human α -synuclein expression (green) in hepatocytes. Liver tissues were harvested 5 months after a single injection of tamoxifen or vehicle in 4-month-old mice. d Western blot analysis of human α -synuclein expression in the blood 3 weeks after tamoxifen or vehicle injection. e Schematic

diagram of the experimental timeline for histological and behavioral assessments of Alb-CreERT2; hSNCA^{se} mice. **f** Wire hanging test showing no significant motor impairment. **g** Grip strength assay demonstrating unchanged motor function. **h**–**j** Quantification of open field test parameters: time spent in the center zone (**h**), total distance traveled (**i**), and distance traveled in the center zone (**j**). No significant differences were observed across any of the parameters. Data are presented as mean \pm SEM. Statistical analysis was performed using unpaired two-tailed Student's t tests; n.s. not significant (P > 0.05). Sample sizes for each group are indicated in parentheses within the graph.

hanging test, grip strength assay, and open field test (Fig. 1e). However, none of these tests revealed any obvious changes in motor function in mice with excess α -synuclein in their blood, despite the fact that such motor changes are typically observed in PD models (Fig. 1f–j). These results suggest that prolonged high levels of α -synuclein exclusively in the blood do not show significant behavioral symptoms observed in PD model.

Given the unexpectedly normal behavioral phenotype, our next investigation aimed to determine whether the substantial increase in blood α -synuclein levels could induce the formation of high-molecular-weight aggregates in blood plasma. We observed a high level of the monomeric form of α -synuclein at 6 months of age, and this level was consistently maintained up to 18 months of age without a further increase (Fig. 2a). However, prolonged induction of α -synuclein secretion did not result in oligomeric α -synuclein in the blood of Alb-CreERT2; hSNCAse mice, whereas brain extracts from a familial PD mouse model (referred to as M83)²¹ revealed the presence of obvious dimers as well as high-molecular-weight oligomeric α -synuclein proteins (Fig. 2a).

We hypothesized that the concentration of α -synuclein in the blood is insufficient to promote aggregation. α-synuclein is known to exhibit prionlike behavior, wherein monomers associate with seed molecules and elongate into larger fibrillar structures²². We first quantified the concentration of α-synuclein in the blood using the ELISA method and found that the concentration of monomeric α-synuclein (≈2.7 μM) in the blood is significantly higher than the previously reported threshold of 0.45 µM required for aggregate formation with seed molecules (Fig. 2b and Supplementary Fig. 2a)²³. To examine whether blood-derived monomeric α-synuclein can form aggregates upon binding to seed molecules, we introduced sonicated pre-formed fibrils (PFFs) into blood samples and performed a thioflavin T (ThT) assay (Supplementary Fig. 2b). Interestingly, secreted monomeric αsynuclein in blood samples did not aggregate upon the addition of PFFs, whereas an equivalent concentration of monomeric α-synuclein in buffer facilitated aggregation (Fig. 2c, d). These results suggest the presence of a protective cellular mechanism that prevents α-synuclein aggregation and toxicity under physiological conditions. Previous studies have reported that certain plasma proteins, such as apolipoprotein A1 (ApoA1) and α2-macroglobulin (A2M), can inhibit α-synuclein aggregation^{24–26}. Therefore, we examined the effects of these plasma aggregation inhibitors in vitro using a ThT assay. ApoA1 dramatically suppressed PFF formation, whereas A2M exhibited a modest but detectable inhibitory effect (Fig. 2d). To further examine whether inhibitory factors in the blood can prevent α-synuclein aggregation in vivo, we intravenously administered α-synuclein PFFs via the retro-orbital route to α-synuclein-overexpressing mice (Supplementary Fig. 3a). Despite this repeated challenges, ThT kinetic assays of plasma samples showed no detectable α-synuclein aggregation (Supplementary Fig. 3b). Moreover, we found no evidence of high-molecular-weight α-synuclein species in either brain or plasma samples (Supplementary Fig. 3c, d), nor any accumulation in the brain parenchyma (Supplementary Fig. 3e). These results further support the notion that plasma-derived inhibitory factors, such as ApoA1 and A2M, effectively suppress α-synuclein aggregation in vivo, thereby preventing the formation of pathological fibrils and their subsequent accumulation in the brain.

Although the monomeric form of α -synuclein is known to be transported bidirectionally between the blood and brain 27 , we detected no human α -synuclein in any region of the brain in aged Alb-CreERT2;hSNCA se mice,

despite prolonged overproduction in the blood (Fig. 2e and Supplementary Fig. 5c). The discrepancy from our in vitro observations (Supplementary Fig. 1d), where α -synuclein was taken up by endothelial cells, may be explained by the highly restrictive nature of the in vivo BBB, along with active clearance mechanisms that limit α -synuclein accumulation at the brain interface. Supporting this, time-course analysis following exogenous α -synuclein injection showed a rapid decrease in α -synuclein levels in peripheral organs such as the kidney, within 2 h (Supplementary Fig. 4a,b). Prolonged α -synuclein expression in the blood also caused selective accumulation in the kidney and, to a lesser extent, the heart (Fig. 2f and Supplementary Fig. 5a), but not in the spleen, stomach, and intestines (Supplementary Fig. 5d–f).

Moreover, previous studies have also suggested that α -synuclein uptake and degradation by immune cells, particularly monocytes, macrophages, and T cells, may contribute to this inhibition 28,29 . To determine whether elevated α -synuclein levels in the blood lead to changes in immune cell composition, we analyzed the proportions of T cells, B cells, and monocytes in peripheral blood mononuclear cells from α -synuclein-over-expressing and control mice. As shown in Supplementary Fig. 6, we found no significant differences between the two groups, suggesting that immune cell composition was not altered in response to elevated blood α -synuclein.

Although no aggregates were observed, we considered the possibility that blood-derived α -synuclein might exert subtle neurotoxic effects without forming detectable aggregates. To investigate this, we performed immunohistochemical staining for tyrosine hydroxylase (TH) to evaluate the integrity of dopaminergic neurons in the substantia nigra, the primary pathological region in PD. As shown in Fig. 2g, h, the number of TH-positive neurons did not differ significantly between α -synuclein-over-expressing mice and controls, indicating no apparent dopaminergic neurodegeneration under our experimental conditions.

Recent studies have shown that α-synuclein proteins in the blood are present in extracellular vesicles derived from erythrocytes and the central nervous system and are efficiently transported through membrane adsorptive transcytosis 18,30,31 . However, the human α -synuclein secreted into the blood by hepatocytes in Alb-CreERT2; hSNCA^{se} mice is not in the encapsulated monomeric form and therefore requires another transport mechanism. Bidirectional transport of α-synuclein across the BBB through direct loading of purified proteins has been reported in rodents²⁷. Radiolabeled α-synuclein can be transported bidirectionally between the blood and brain following intracerebroventricular or intravenous injection, and this transport from brain to blood involves LRP1mediated transcytosis²⁷. In addition, various forms of α -synuclein aggregates can cross the BBB after intravenous injection, leading to synucleinopathies³². Recent in vitro studies have shown that brain endothelial cells internalize the monomeric form of α -synuclein through a clathrin-dependent mechanism, allowing bidirectional transport³³. In contrast to these studies, we did not detect any human α-synuclein in brain endothelial cells or the parenchyma (Fig. 2e). These results could be due to the efficient elimination of exogenous α -synuclein via endothelial cells in healthy animals or the prevention of α -synuclein entry into the brain by plasma proteins. Given that pathological inflammation can disrupt the BBB and facilitate the uptake of α -synuclein²⁷, it would be valuable to investigate the mechanisms underlying the blood-to-brain transport of α -synuclein under different disease conditions.

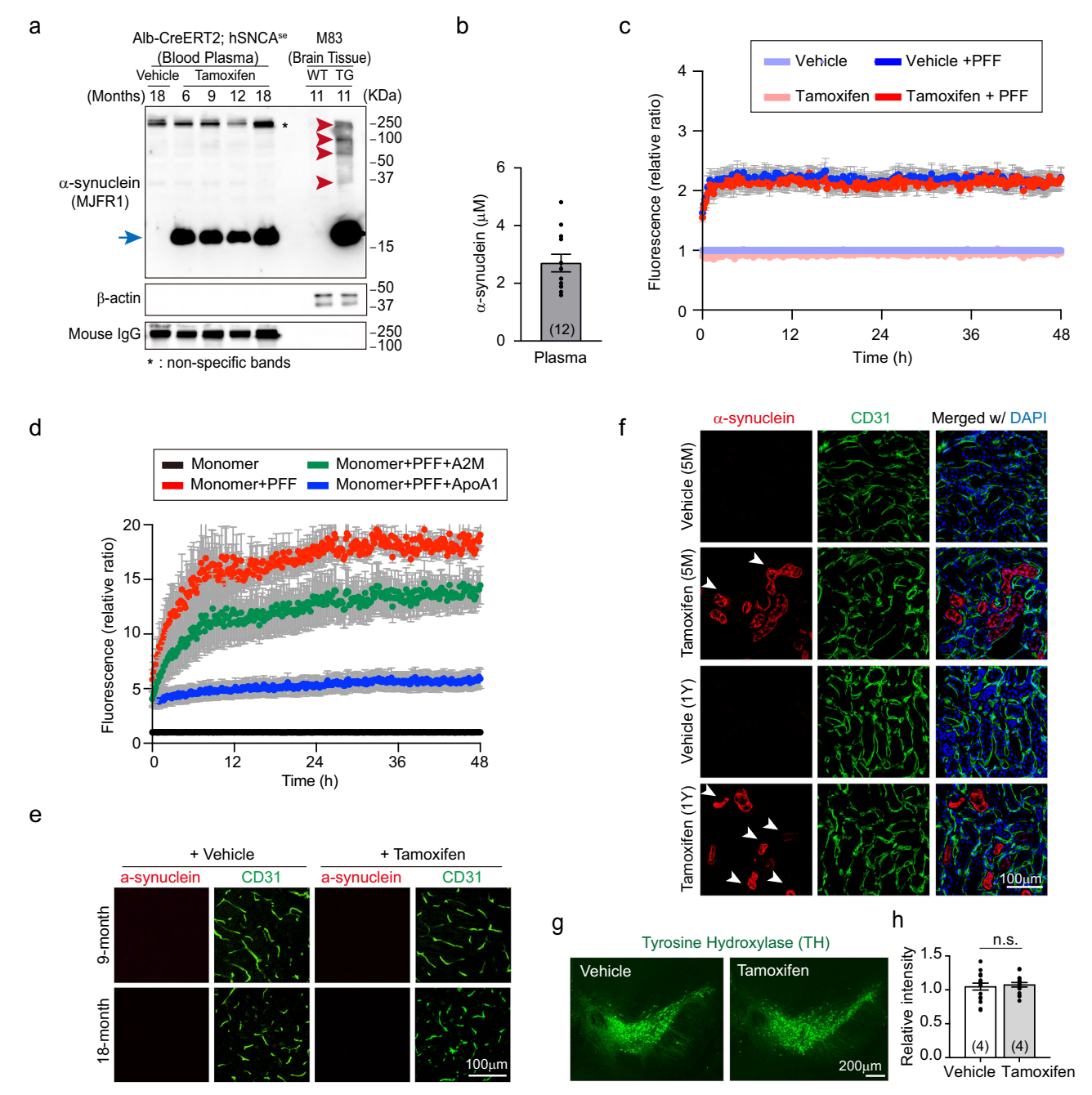


Fig. 2 | Elevated circulating human α-synuclein does not trigger pathological progression. a Western blot analysis of human α-synuclein in blood plasma (50 μg) from tamoxifen-injected Alb-CreERT2; hSNCA* mice, and brain extracts (5 μg) from M83 mice expressing human A53T α-synuclein (red arrowhead). The asterisk denotes a nonspecific band. b Quantification of α-synuclein levels in blood plasma using ELISA. The standard curve is shown in Supplemental Fig. 2. c Thioflavin T (ThT) kinetic seeding assay of blood plasma from Vehicle- and Tamoxifen-injected Alb-CreERT2; hSNCA* mice with or without 2 μM sonicated PFFs (n = 5 per group; freshly prepared samples (n = 2) and frozen samples (n = 3)). Note that brain immunostaining from these animals shows negative results for human α-synuclein. d The kinetic seeding assay under buffer-based in vitro conditions. α2-macroglobulin (A2M, 0.06 μM, green) or apolipoprotein A1 (ApoA1, 1.5 μM, blue) was added to assess inhibitory effects on fibril formation (n = 5 per group). Symbols

represent the mean, and error bars indicate the standard error of multiple experiments in (\mathbf{c} , \mathbf{d}). \mathbf{e} Representative immunostaining images of the cortex showing human α -synuclein (red) and the endothelial marker CD31 (green) in brain sections from 9-month-old and 18-month-old Alb-CreERT2; hSNCA* mice (n=4 per group). \mathbf{f} Representative immunostaining images showing α -synuclein deposition in the kidney tissues of Alb-CreERT2; hSNCA* mice at 5 months (n=1 per group) and 1 year of age (vehicle, n=2; tamoxifen, n=3). Both age groups received tamoxifen (or corn oil) induction at 4 months of age and were sacrificed at the indicated time points. Immunostaining was performed using a human α -synuclein antibody (red) and the endothelial marker CD31 (green). \mathbf{g} Representative immunostaining images showing tyrosine hydroxylase (TH, green). \mathbf{h} Quantification of TH signal shown in (\mathbf{g}) (n=4 mice per group (seven sections/mouse)).

Various animal models have been developed to investigate the progression of PD. These models involve the specific ablation of dopaminergic neurons through toxin-induced methods or manipulation of PD-related genes, including α -synuclein^{34–36}. Although these models are widely used at

present, they still face limitations in accurately recapitulating the pathological symptoms of PD observed in human patients. The development of these models is particularly challenging because of the diverse pathological factors underlying idiopathic PD, which is the most prevalent type of PD. To

accurately elucidate the mechanism underlying PD progression in human patients, more targeted disease models need to be developed.

Previous studies have shown that both the monomeric and oligomeric forms of α -synuclein can be released into the extracellular space through unconventional exocytosis, which may lead to the propagation of α -synuclein ^{37,38}. From these perspectives, our hSNCA^{se} mouse model, which allows precise spatial and temporal control of extracellular α -synuclein upregulation, is highly valuable for investigating the mechanism of intercellular α -synuclein spreading. Surprisingly, in the present study utilizing the hSNCA^{se} mouse model, we did not observe any significant pathological evidence explaining the selective increase in α -synuclein levels in the blood, suggesting that hSNCA^{se} mice will enable us to study in detail the various roles of extracellular α -synuclein in different tissues or cells and the related mechanisms through crossbreeding with mice expressing specific Cre drivers

Methods

Mouse models

M83 transgenic mice (JAX stock #004479) and Alb-CreERT2 mice were purchased from the Jackson Laboratory (Bar Harbor, USA) and Shanghai Model Organisms Center, Inc. (Shanghai, China), respectively. To generate hSNCA^{se} mice, a construct targeting secretable human α-synuclein was designed as illustrated in Fig. 1a, with a modified human albumin signal peptide added to the 5' end of the α-synuclein cDNA and a floxed stop cassette inserted for conditional expression. The construct was introduced into the ROSA26 locus via CRISPR-Cas9, and mouse generation was verified by Biocytogen (Waltham, MA, USA). All mice were maintained on a C57BL/6 J background (JAX stock #000664) and housed under standard conditions with a 12-h light/dark cycle. Alb-creERT2;hSNCAse mice were injected with tamoxifen (0.1 mg/g) to induce α-synuclein expression via oral gavage; control mice received corn oil in the same manner. All protocols for animal experiments were approved by the Institutional Animal Care and Use Committee of Korea Brain Research Institute (IACUC-19-00001, IACUC-23-00011, and IACUC-24-00047). All experiments were performed according to the National Institutes of Health Guide for the Care and Use of Laboratory Animals and ARRIVE guidelines.

Blood plasma sampling

Mice were anesthetized with avertin (125 mg/kg), and blood was collected by cutting the right atrium using a syringe pre-coated with 0.5 M ethylenediaminetetraacetic acid (EDTA). Plasma samples were transferred to microcentrifuge tubes and incubated at room temperature (RT) for 10-15 min. The samples were then centrifuged at $2000 \times g$ for 10 min at 4 °C, and the supernatant was transferred to a new microcentrifuge tube for immediate use or stored at -80 °C up to 9 months.

Plasmid and cloning

The pcDNA3.1-sfCherry (1–10) vector (Addgene, #70222) was generously provided by Dr. Hyungju Park (Korea Brain Research Institute). To generate secretable hSNCA, 536-bp gene containing N-terminal KpnI and C-terminal NotI restriction sites (Albumin signal peptide-myc-hSNCA) was synthesized and inserted into pBHA vector (Bioneer Gene Synthesis service) as illustrated in Supplementary Fig. 1a. The final secretable hSNCA construct was formed by inserting the synthetic gene into the KpnI/NotI site in pcDNA3.1-sfCherry (1–10) vector. For the non-secretable hSNCA, the myc-hSNCA sequence was amplified by PCR from the secretable hSNCA gene and the amplified gene was inserted into the KpnI/NotI site in pcDNA3.1-sfCherry (1–10) vector. The DNA sequences of each construct were confirmed by sequencing before use.

Cell culture and transfection

Human hepatoma HepG2 cells, kindly provided by Dr. Jung-Woong Kim (Chung-Ang University), and mouse brain endothelial bEnd.3 cells (ATCC, CRL-2299) were cultured at 37 °C in a humidified incubator with 5% $\rm CO_2$ in Dulbecco's Modified Eagle Medium (DMEM) supplemented with 10% fetal

bovine serum (FBS) and 100 U/ml penicillin-streptomycin. Plasmid constructs (4 μ g) were transfected into cultured cells (3 × 10⁴ cells/cm²) using Lipofectamine 2000 (Invitrogen, #11668019) in OPTI-MEM (Gibco, #31985-070) for 4 h, following the manufacturer's protocol.

Conditioned media preparation

Cultured media from HepG2 cells transfected with vector, myc-tagged secretable and non-secretable human α -synuclein constructs were collected 48 h after transfection. The media were centrifuged at $500 \times g$ for 10 min to remove dead cells. The supernatants were then transferred to new conical tubes and further centrifuged at $3000 \times g$ for 20 min to eliminate cell debris.

Protein sample preparation

The culture media were collected and centrifuged at 12,000 rpm for 5 min to remove the debris. The cells were washed with ice-cold phosphate-buffered saline (PBS, pH 7.4) and harvested using ice-cold lysis buffer [50 mM Tris-HCl (pH 7.5), 150 mM NaCl, 30 mM MgCl $_2$, 1% Nonidet P-40, and 1 mM dithiothreitol (DTT)] supplemented with a mixture of protease and phosphatase inhibitors. The lysates were incubated on ice for 20 min and then centrifuged at 12,000 rpm for 5 min at 4 $^{\circ}\mathrm{C}$.

For brain extracts, mice were perfused with ice-cold PBS and the brains were homogenized on ice in lysis buffer [50 mM Tris-HCl (pH 7.4), 175 mM NaCl, 5 mM EDTA] supplemented with protease and phosphatase inhibitors using a Taco Prep Bead Beater (GeneReach, Biotechnology Corp., Taiwan). Triton X-100 was added to the homogenates to a final concentration of 1%, and the mixture was incubated on ice for 30 min. The homogenates were then centrifuged at $15,000 \times g$ for 1 h. The protein concentrations were determined using a Pierce BCA Protein Assay Kit (Thermo Fisher Scientific, #23225).

Western blotting

For western blot analysis of cell lysates and culture media, 30 µg of protein was separated on a 12% SDS-PAGE gel and transferred to a polyvinylidene fluoride (PVDF) membrane. For mouse samples, 50 µg of blood plasma and 5 µg of brain homogenates were subjected to 12% SDS-PAGE and transferred to a nitrocellulose or PVDF membrane. The protein samples were diluted in 5× sample buffer [250 mM Tris-HCl (pH 6.8), 8% sodium dodecyl sulfate, 0.1% bromophenol blue, 40% glycerol, 100 mM DTT]. The non-reducing sample buffer did not contain DTT. Membranes were blocked with 5% skim milk in Tris-buffered saline containing 0.1% Tween-20 (TBS-T) for 1 h and then incubated with the primary antibodies listed below in the same blocking buffer at 4 °C overnight (O/N). The primary antibodies used were anti-α-synuclein (MJFR1) (1:5000, Abcam, #138501) and anti-β-actin (1:5,000, Cell Signaling, #5125). After incubation with the appropriate horseradish peroxidase-conjugated secondary antibodies, the protein bands were visualized using enhanced chemiluminescence on FusionFX7 (Vilber, Germany).

Preparation of α-synuclein fibril and Thioflavin T assay

To prepare seed fibrils, $300 \, \mu l$ of 1 mg/ml monomeric α -synuclein solution (purchased from NKMAX Co., Republic of Korea) was incubated at 37 °C with continuous shaking at 1050 rpm (Thermomixer C, Eppendorf) for 48 h. The resulting fibrils were used immediately or saved up to a few days at 4 °C to prevent repeated freeze-thaw cycles. For thioflavin T kinetics, the fibrils were sonicated on ice for 60 s at 20% amplitude using 1 s on/off cycles (total duration: 2 min). Fibril fragmentation was confirmed using a transmission electron microscope (Tecnai G2) after sonication. To assess α -synuclein aggregation in mice, $10 \, \mu g$ of PFFs were retro-orbitally injected.

Amyloid formation was measured using a FLUOstar Omega microplate reader (BMG LABTECH) with Omega software (version 5.50 R4). Samples were prepared in a 96-well black plate (Greiner, #655096). Plasma samples (20 μ g) were diluted in PBS, adding 10 μ M of Thioflavin T solution. Fluorescence (λ ex/em = 440/480 nm) was recorded at 37 °C every 10 min with double orbital shaking at 500 rpm for 10 s prior to each measurement.

To monitor α -synuclein fibril formation under buffer-based conditions (6 mM pH 7.2 NaPO₄ buffer, 140 mM NaCl, 10 mM NaN₃, and 1 mM EDTA), 3 μ M of synthetic α -synucleins (ATGen, #SNA2001L) was used in place of plasma samples. To assess the inhibitory effect on fibril formation, human apolipoprotein A1 (1.5 μ M; Sigma, A0722) and α 2-macrogobulin (0.06 μ M; Sigma, M6159) were added to the mixture. The rest of the experimental setup remained the same as for plasma samples.

Enzyme-linked immunosorbent assay (ELISA)

Plasma α-synuclein levels in Alb-CreERT2; hSNCA^{se} mice were quantified using a commercial ELISA Kit (LEGEND MAXTM Human α-synuclein, colorimetric, BioLegend, #448607). Plasma samples were diluted 1:5000 in PBS. The diluted samples were then incubated according to the manufacturer's instructions to ensure optimal binding and detection of α-synuclein levels in the plasma.

Immunocytochemistry

bEnd.3 cells were fixed in 4% paraformaldehyde (PFA) in PBS for 5 min, followed by two washes with PBS. Cells were permeabilized in PBST (PBS containing 0.1% Triton X-100) for 5 min. Blocking was performed using 5% horse serum in PBST for 60 min at RT. Cells were incubated O/N at 4 °C with anti-Myc antibody (1:1,000, Cell Signaling, #2276S) diluted in blocking solution. The next day, after three washes in PBST (PBS containing 0.2% Tween-20), the cells were incubated for 1 h at RT with Alexa Fluor 594-conjugated secondary antibodies (1:500, Invitrogen, A32758) and 1 μ g/ml of DAPI (Sigma-Aldrich, D9542). The samples were then washed three times with 0.2% PBST, mounted with ProLong[™] Diamond Antifade Mountant (Invitrogen, #P36962), and analyzed using a Leica TCS SP8 confocal microscope (Leica, Germany).

Immunohistochemistry

Mice were anesthetized with avertin (125 mg/kg) and transcardially perfused with PBS followed by 4% PFA in PBS. The brains and peripheral tissues (heart, stomach, intestine, liver, kidney, and spleen) were promptly removed and post-fixed in 4% PFA/PBS at 4 °C, O/N for brains and 1 h for peripheral tissues. After fixation, the tissues were rinsed three times with PBS and then incubated in 30% sucrose in PBS. The tissues were then embedded in optimal cutting temperature compound (Leica BIOSYSTEMS, #3801480), and stored at $-80\,^{\circ}\mathrm{C}$ until sectioning for further analysis.

For immunostaining of brain sections, 30 μ m thick slices were cut using a cryostat (Leica Microsystems, Inc.). The sections were rinsed with PBS and permeabilized in PBST (PBS containing 0.2% Triton X-100) for 5 min, followed by blocking with 1% bovine serum albumin (BSA) supplemented with 0.3 M glycine in 0.2% PBST for 1 h at RT. And then, primary antibodies diluted in 1% BSA/0.2% PBST solution were applied to brain slices and incubated O/N at 4 °C. Following three washes with 0.2% PBST, the sections were incubated with Alexa Fluor 488- and 594-conjugated secondary antibodies (1:1000; Invitrogen) and 1 μ g/ml of DAPI (Sigma-Aldrich, D9542) in 0.2% PBST for 1 h. The sections were then washed three times with 0.2% PBST, mounted with ProLong[™] Diamond Antifade Mountant (Invitrogen, #P36962), and analyzed by imaging.

For immunostaining of peripheral tissues, the same protocol was followed with minor adjustments. Tissues were cut at $14\,\mu m$ thickness and mounted onto glass slides. The slides were rinsed with PBS and permeabilized with 0.3% PBST for 15 min. The sections were then incubated with a blocking buffer (10% donkey serum and 0.3 M glycine in 0.2% PBST). Primary and secondary antibodies were dissolved in an antibody solution (2% donkey serum in 0.2% PBST). The following primary antibodies were used at the indicated dilutions for both brains and peripheries: anti- α -synuclein (MJFR1, 1:5000, Abcam, #138501)), anti-tyrosine hydroxylase (1:500, Pel-Freez Biologicals, #P60101-150) and anti-CD31 (1:150, BD Bioscience, #553370). To reduce nonspecific autofluorescence in aged tissue samples, sections were treated with $1\times$ TrueBlack solution (Biotium,

#23007) diluted in 70% ethanol for 30 s, followed by thorough PBS washes. Images were acquired with a Leica TCS SP8 confocal microscope (Leica, Germany) and NiKon A1 Rsi/Ti-E (Nikon, Japan). All image processing was performed using Fiji (ImageJ) and Adobe Photoshop (Adobe Photoshop CC2022) software.

Flow cytometry

Peripheral blood was obtained from the retro-orbital vein of mice and transferred into tubes containing 50 µL of 0.5 M EDTA. Red blood cells were lysed using RBC lysis buffer (Thermo Fisher Scientific, #00-4333-57), and the remaining cells were washed with RPMI1640 medium (WELGENE, South Korea) supplemented with 10% fetal bovine serum (FBS; HyClone, USA) and 1× antibiotic-antimycotic solution (Gibco, USA). The resulting cell pellet was resuspended in flow cytometry buffer (PBS containing 2% FBS and 1 mM EDTA). Cell suspensions were then incubated with antimouse CD16/CD32 (Fc receptor blocker; BD Biosciences, #553142) at room temperature for 15 min. Surface antigens were stained with fluorochromeconjugated antibodies at 4 °C for 15 min. The following antibodies were used: APC anti-CD45R (B220) (#17-0452-82), APC-eFluor780 anti-CD3e (#47-0032-82), PerCP-Cy5.5 anti-CD11b (#45-0112-82), and PE anti-Ly6G (#12-5931-81; all from Thermo Fisher Scientific). Stained cells were analyzed using an Attune NxT flow cytometer (Thermo Fisher Scientific, USA), and data were processed using FlowJo software (BD Biosciences, USA).

Behavioral analysis

All behavior tests were performed when the mice reached 9 months of age. Prior to testing, the mice underwent a 5-minute handling session for three consecutive days, followed by a one-day rest period before the actual tests. On the testing day, the mice were habituated to the testing room for at least 1 h. The open field test was performed first to minimize the effects of stress. This was followed by the grip strength and wire hanging tests, which were conducted with a one-week interval between them. To minimize the influence of odor cues, all the apparatuses were thoroughly cleaned with 70% ethanol after each trial.

(i) Wire hanging test

To evaluate muscle strength, a chamber with a wire lid (30 cm width \times 26 cm length \times 24 cm height) was used. The mice were placed on the lid, and the chamber was gently shaken to encourage the mice to grasp the wire. The lid was then inverted, and the time taken for the mouse to fall was recorded, with a maximum recording time of 2 min.

(ii) Grip strength assay

Forelimb grip strength was measured using a grip strength meter (Ugo Basile Company, #47200-001). The mice were gently held by the tail and positioned on a grip bar. Then, the tail was steadily pulled backward until the mouse released its grip on the bar. Grip strength was measured twice, and the average of the two measurements was used for analysis.

(iii) Open field test

To assess locomotion and anxiety-related behavior, the mice were placed in the center of an open field apparatus (40 cm width \times 40 cm length \times 40 cm height). Their movements were recorded using a video camera for 20 min. Parameters such as the total distance traveled, distance traveled within the center zone, and time spent in the center zone were analyzed using video tracking software (SMART3.0, Panlab). The experiments were conducted in soundproof, closed chambers to minimize external disturbances.

Statistical analysis

Statistical analyses were performed using GraphPad Prism 9.5.1 (GraphPad Software, Inc.). All values are presented as the mean \pm standard error of the mean (SEM). All data were subjected to and passed the Shapiro-Wilk normality test. To test for statistical significance between two groups, unpaired two-tailed Student's t tests were used.

Data availability

All data used in this study and materials, including mouse models, are available upon request.

Received: 24 January 2025; Accepted: 23 July 2025; Published online: 04 August 2025

References

- Lashuel, H. A., Overk, C. R., Oueslati, A. & Masliah, E. The many faces of α-synuclein: from structure and toxicity to therapeutic target. *Nat. Rev. Neurosci.* 14, 38–48 (2013).
- Bogale, T. A. et al. Alpha-synuclein in the regulation of brain endothelial and perivascular cells: gaps and future perspectives. Front. Immunol. 12, 611761 (2021).
- Wolfson, L. I., Leenders, K. L., Brown, L. L. & Jones, T. Alterations of regional cerebral blood flow and oxygen metabolism in Parkinson's disease. Neurology 35, 1399 (1985).
- Gray, M. T. & Woulfe, J. M. Striatal blood–brain barrier permeability in Parkinson's disease. *J. Cereb. Blood Flow. Metab.* 35, 747–750 (2015).
- Ham, J. H. et al. Cerebral microbleeds in patients with Parkinson's disease. J. Neurol. 261, 1628–1635 (2014).
- Biju, K., Shen, Q., Hernandez, E. T., Mader, M. J. & Clark, R. A. Reduced cerebral blood flow in an α-synuclein transgenic mouse model of Parkinson's disease. *J. Cereb. Blood Flow. Metab.* 40, 2441–2453 (2019).
- Barcia, C. et al. Changes in vascularization in substantia nigra pars compacta of monkeys rendered parkinsonian. *J. Neural Transm.* 112, 1237–1248 (2005).
- Kim, T. et al. Poststroke induction of α-synuclein mediates ischemic brain damage. J. Neurosci. 36, 7055–7065 (2016).
- Elabi, O. et al. Human α-synuclein overexpression in a mouse model of Parkinson's disease leads to vascular pathology, blood brain barrier leakage and pericyte activation. Sci. Rep. 11, 1120 (2021).
- 10. Guan, J. et al. Vascular degeneration in Parkinson's disease. *Brain Pathol.* **23**, 154–164 (2012).
- Jeong, J.-Y. et al. Impaired neuronal activity as a potential factor contributing to the underdeveloped cerebrovasculature in a young Parkinson's disease mouse model. Sci. Rep. 13, 22613 (2023).
- 12. Tamo, W. et al. Expression of α -synuclein, the precursor of non-amyloid β component of Alzheimer's disease amyloid, in human cerebral blood vessels. *Neurosci. Lett.* **326**, 5–8 (2002).
- Nakai, M. et al. Expression of α-synuclein, a presynaptic protein implicated in Parkinson's disease, in erythropoietic lineage. *Biochem. Biophys. Res. Commun.* 358, 104–110 (2007).
- Barbour, R. et al. Red blood cells are the major source of alphasynuclein in blood. Neurodegener. Dis. 5, 55–59 (2008).
- Zubelzu, M., Morera-Herreras, T., Irastorza, G., Gómez-Esteban, J. C. & Murueta-Goyena, A. Plasma and serum alpha-synuclein as a biomarker in Parkinson's disease: a meta-analysis. *Park. Relat. Disord.* 99, 107–115 (2022).
- El-Agnaf, O. M. A. et al. Detection of oligomeric forms of α-synuclein protein in human plasma as a potential biomarker for Parkinson's disease. FASEB J. 20, 419–425 (2006).
- 17. Zhao, H.-Q., Li, F., Wang, Z., Wang, X.-M. & Feng, T. A comparative study of the amount of α-synuclein in ischemic stroke and Parkinson's disease. *Neurol. Sci.* **37**, 749–754 (2016).
- Kluge, A. et al. Detection of neuron-derived pathological α-synuclein in blood. Brain 145, 3058–3071 (2022).
- Attallah, C., Etcheverrigaray, M., Kratje, R. & Oggero, M. A highly efficient modified human serum albumin signal peptide to secrete proteins in cells derived from different mammalian species. *Protein Expr. Purif.* 132, 27–33 (2017).
- He, L. et al. Enhancing the precision of genetic lineage tracing using dual recombinases. *Nat. Med.* 23, 1488–1498 (2017).

- Giasson, B. I. et al. Neuronal α-synucleinopathy with severe movement disorder in mice expressing A53T human α-synuclein. Neuron 34, 521–533 (2002).
- Vargas, J. Y., Grudina, C. & Zurzolo, C. The prion-like spreading of α-synuclein: From in vitro to in vivo models of Parkinson's disease.
 Ageing Res. Rev. 50, 89–101 (2019).
- Afitska, K., Fucikova, A., Shvadchak, V. V. & Yushchenko, D. A. α-Synuclein aggregation at low concentrations. *Biochim. Biophys.* Acta 1867, 701–709 (2019).
- Zhou, Y. et al. Analysis of α-synuclein-associated proteins by quantitative proteomics* [boxs]. J. Biol. Chem. 279, 39155–39164 (2004).
- Whiten, D. R. et al. Single-molecule characterization of the interactions between extracellular chaperones and toxic α-synuclein oligomers. *Cell Rep.* 23, 3492–3500 (2018).
- Bellomo, G. et al. Cerebrospinal fluid lipoproteins inhibit α-synuclein aggregation by interacting with oligomeric species in seed amplification assays. *Mol. Neurodegener.* 18, 20 (2023).
- Sui, Y.-T., Bullock, K. M., Erickson, M. A., Zhang, J. & Banks, W. A. Alpha synuclein is transported into and out of the brain by the blood-brain barrier. *Peptides* 62, 197–202 (2014).
- 28. Tansey, M. G. et al. Inflammation and immune dysfunction in Parkinson disease. *Nat. Rev. Immunol.* **22**, 657–673 (2022).
- Matveyenka, M., Zhaliazka, K. & Kurouski, D. Macrophages and natural killers degrade α-synuclein aggregates. *Mol. Pharm.* 21, 2565–2576 (2024).
- Matsumoto, J. et al. Transmission of α-synuclein-containing erythrocyte-derived extracellular vesicles across the blood-brain barrier via adsorptive mediated transcytosis: another mechanism for initiation and progression of Parkinson's disease?. Acta Neuropathol. Commun. 5, 71 (2017).
- Shi, M. et al. Plasma exosomal α-synuclein is likely CNS-derived and increased in Parkinson's disease. Acta Neuropathol. 128, 639–650 (2014).
- 32. Peelaerts, W. et al. α-synuclein strains cause distinct synucleinopathies after local and systemic administration. *Nature* **522**, 340–344 (2015).
- Alam, P. et al. Polarized α-synuclein trafficking and transcytosis across brain endothelial cells via Rab7-decorated carriers. Fluids Barriers CNS 19, 37 (2022).
- Aniszewska, A., Bergström, J., Ingelsson, M. & Ekmark-Lewén, S. Modeling Parkinson's disease-related symptoms in alpha-synuclein overexpressing mice. *Brain Behav.* 12, e2628 (2022).
- Breger, L. S. & Armentero, M. T. F. Genetically engineered animal models of Parkinson's disease: from worm to rodent. *Eur. J. Neurosci.* 49, 533–560 (2019).
- Przedborski, S. & Vila, M. The 1-methyl-4-phenyl-1,2,3,6-tetrahydropyridine mouse model: a tool to explore the pathogenesis of Parkinson's disease. *Ann. N. Y. Acad. Sci.* 991, 189–98 (2003).
- Lee, H.-J., Patel, S. & Lee, S.-J. Intravesicular localization and exocytosis of α-synuclein and its aggregates. *J. Neurosci.* 25, 6016–6024 (2005).
- Wu, S. et al. Unconventional secretion of α-synuclein mediated by palmitoylated DNAJC5 oligomers. eLife 12, e85837 (2023).

Acknowledgements

We thank Drs. Sangjune Kim and Soonmoon Yoo for reading the manuscript and providing critical advice; Dr. Jung-Woong Kim for providing HepG2 cells; the Brain Research Core Facilities in KBRI for image analysis. This research was supported by the KBRI basic research program of the Korea Brain Research Institute funded by the Ministry of Science and ICT (KBRI 24-BR-01-02, 25-BR-01-02, 25-BR-05-06), and the Bio & Medical Technology Development Program of the NRF funded by the Korean government (MSIT) (NRF-2020M3E5D9079766 and NRF-2022M3E5E8017701) to W.O.

Author contributions

Conceptualization, funding acquisition, project administration, supervision, and writing–original draft: W.J.O. Data curation and writing–review & editing: J.Y.J., N.K. Formal analysis: W.J.O., J.Y.J., N.K., D.J.K, and Y.L. Providing materials and technical advice: H.K.K., D.J.K. Analysis: J.Y.J., N.K. D.J.K. All authors read and approved the final manuscript.

Competing interests

The authors declare no competing interests.

Additional information

Supplementary information The online version contains supplementary material available at https://doi.org/10.1038/s41531-025-01091-z.

Correspondence and requests for materials should be addressed to Won-Jong Oh.

Reprints and permissions information is available at http://www.nature.com/reprints

Publisher's note Springer Nature remains neutral with regard to jurisdictional claims in published maps and institutional affiliations.

Open Access This article is licensed under a Creative Commons Attribution-NonCommercial-NoDerivatives 4.0 International License, which permits any non-commercial use, sharing, distribution and reproduction in any medium or format, as long as you give appropriate credit to the original author(s) and the source, provide a link to the Creative Commons licence, and indicate if you modified the licensed material. You do not have permission under this licence to share adapted material derived from this article or parts of it. The images or other third party material in this article are included in the article's Creative Commons licence, unless indicated otherwise in a credit line to the material. If material is not included in the article's Creative Commons licence and your intended use is not permitted by statutory regulation or exceeds the permitted use, you will need to obtain permission directly from the copyright holder. To view a copy of this licence, visit http://creativecommons.org/licenses/bync-nd/4.0/.

© The Author(s) 2025